The Hydrologic Effects of Synchronous El Niño–Southern Oscillation and Subtropical Indian Ocean Dipole Events over Southern Africa

ANDREW HOELL

NOAA/Earth System Research Laboratory/Physical Sciences Division, Boulder, Colorado

ANDREA E. GAUGHAN

Department of Geography and Geosciences, University of Louisville, Louisville, Kentucky

SHRADDHANAND SHUKLA

Department of Geography, University of California, Santa Barbara, Santa Barbara, California

TAMUKA MAGADZIRE

Famine Early Warning Systems Network, Gabarone, Botswana

(Manuscript received 23 December 2016, in final form 27 June 2017)

ABSTRACT

Southern Africa precipitation during December–March (DJFM), the height of the rainy season, is closely related with two modes of climate variability, El Niño–Southern Oscillation (ENSO) and the subtropical Indian Ocean dipole (SIOD). Recent research has found that the combined effects of ENSO and SIOD phasing are linked with changes to the regional southern Africa atmospheric circulation beyond the individual effects of either ENSO or SIOD alone. Here, the authors extend the recent research and examine the southern Africa land surface hydrology associated with the synchronous effects of ENSO and SIOD events using a macroscale hydrologic model, with particular emphasis on the evolution of the hydrologic conditions over three critical Transfrontier Conservation Areas: the Kavango–Zambezi Conservation Area, the Greater Limpopo Transfrontier Park, and the Kgalagadi Transfrontier Park. A better understanding of the climatic effects of ENSO and SIOD phase combinations is important for regional-scale transboundary conservation planning, especially for southern Africa, where both humans and wildlife are dependent on the timing and amount of precipitation. Opposing ENSO and SIOD phase combinations (e.g., El Niño and a negative SIOD or La Niña and a positive SIOD) result in strong southern Africa climate impacts during DJFM. The strong instantaneous regional precipitation and near-surface air temperature anomalies during opposing ENSO and SIOD phase combinations lead to significant soil moisture and evapotranspiration anomalies in the year following the ENSO event. By contrast, when ENSO and SIOD are in the same phase (e.g., El Niño and a positive SIOD or La Niña and a negative SIOD), the southern Africa climate impacts during DJFM are minimal.

1. Introduction

Southern Africa precipitation during December–March (DJFM), the height of the rainy season, is closely related with variations of the El Niño–Southern Oscillation (ENSO; e.g., Nicholson and Entekhabi 1986; Manatsa et al. 2015) and the subtropical Indian Ocean dipole (SIOD; Behera et al. 2000; Behera and Yamagata 2001; Reason 2001; Washington and Preston 2006) modes of climate variability. Further, recent research has shown that the combined effects of ENSO and SIOD phasing are linked with an intensification of the southern Africa precipitation anomalies beyond the individual effects of either ENSO or SIOD alone (Hoell et al. 2016). Despite the implications of ENSO and SIOD phasing on southern Africa floods and droughts, there remains a gap in understanding about how ENSO, SIOD, or their synchronous behavior is linked with the land surface hydrology of the region. The

Corresponding author: Andrew Hoell, andrew.hoell@noaa.gov

DOI: 10.1175/JHM-D-16-0294.1

influence of these climate modes on precipitation anomalies will influence wildlife movement and agricultural land-use decisions, as well as other sustainable livelihood activities dependent on the land surface hydrology (e.g., fishing, harvesting of natural resources). To identify how these two climate modes interact to drive land surface hydrologic patterns at the regional scale, we investigate the synchronous effects of ENSO and SIOD events across southern Africa using simulated hydrologic outputs from a macroscale hydrologic model, with particular emphasis on the evolution of the hydrologic conditions over critical Transfrontier Conservation Areas (TFCAs), where management of human–wildlife interactions is paramount.

ENSO is composed of two phases, El Niño and La Niña, and both are on average related with anomalous atmospheric circulation and precipitation patterns over southern Africa (Nicholson and Entekhabi 1986; Lindesay 1988; Jury et al. 1994; Rocha and Simmonds 1997; Nicholson and Kim 1997; Reason et al. 2000; Misra 2003). The origins of the causal chain in which El Niño and La Niña force southern Africa climate begins with tropical Pacific sea surface temperatures (SSTs). Tropical Pacific SSTs associated with ENSO events drive changes in the tropical Indo-Pacific convection, which in turn release energy to the atmosphere that excite Rossby waves over southern Africa (Ratnam et al. 2014; Hoell et al. 2015). The Rossby waves over southern Africa thereby modify the regional flux of moisture (Reason and Jagadheesha 2005; Hoell et al. 2015) and vertical motions (Hoell et al. 2015), which in turn result in anomalous precipitation patterns (Nicholson and Kim 1997). On average, El Niño is related with anomalously low precipitation, and La Niña is related with anomalously high precipitation over large parts of southern Africa. The relationship between El Niño, La Niña, and southern Africa climate is strongest during DJFM (Manatsa et al. 2015), the rainiest time of year for the region, the reason for which DJFM is the primary focus season in this and previous studies (e.g., Hoell et al. 2016).

Indian, Pacific, and even Atlantic Ocean SST patterns vary from one ENSO event to the next, and each of those SST configurations have different impacts on southern Africa climate. Here we focus specifically on the synchronous behavior of ENSO and the SIOD, but we recognize that the atmosphere–ocean coupling during ENSO events will exert an effect on Atlantic SST, which in turn can provide for an enhanced effect on southern Africa. For example, the atmospheric circulation during ENSO events forces the South Atlantic anticyclone and therefore South Atlantic SSTs, which in turn provide additional forcing to southern Africa climate (e.g., Colberg et al. 2004). Recognizing the various SST patterns associated with ENSO, Ratnam et al. (2014) and Hoell et al. (2015) analyzed the effect of those historical SST patterns during El Niño and La Niña events on southern Africa climate. Both of these studies came to similar conclusions, in that SST anomalies over the east-to-central Pacific during El Niño and La Niña are related with stronger precipitation anomalies over southern Africa. Further work has shown that Indian Ocean SST patterns are modified by the Indian Ocean dipole (Saji et al. 1999) and the SIOD (Behera et al. 2000; Behera and Yamagata 2001) modes of climate variability, and these two climate modes affect Indian Ocean SSTs during all ENSO states. It has been shown that Indian Ocean SST variations as a result of only the SIOD affect southern Africa (Hoell et al. 2016). SST anomalies associated with the SIOD modify the regional circulation, moisture fluxes, and therefore precipitation (Reason 2001; Washington and Preston 2006).

Until recently, the relative effects of the SIOD and ENSO on southern Africa climate were unknown. Manatsa et al. (2011, 2012) attempted to separate the effects of the Indian Ocean and the Pacific Ocean during ENSO using observed data but had limited success because of potential changes to the behavior of the atmospheric circulation in the 1970s and 1990s. More recently, Hoell et al. (2016) used a large ensemble of atmospheric model simulations forced by time-varying SST to successfully decouple the effects of ENSO and the SIOD on southern Africa climate. Through linear regression of precipitation and winds, Hoell et al. (2016) found that when ENSO and SIOD are in opposing phases (e.g., El Niño and a negative SIOD or La Niña and a positive SIOD), then the ENSO and SIOD atmospheric responses are complimentary and result in strong southern Africa climate impacts relative to what typically occurs during ENSO alone. By contrast, Hoell et al. (2016) also found that when ENSO and SIOD are in the same phase (e.g., El Niño and a positive SIOD or La Niña and a negative SIOD), then the ENSO and SIOD atmospheric responses interfere with one another and result in weaker southern Africa impacts relative to what typically occurs during ENSO alone. While the analysis of Hoell et al. (2016) indicates that there is a linear component to the combined effects of ENSO and SIOD over southern Africa, some of the early works on the nonlinearity of ENSO teleconnections (e.g., Hoerling et al. 1997, 2001; DeWeaver and Nigam 2002) motivate us to examine the southern Africa response

to each of the four ENSO and SIOD phase combinations to test the degree of linearity of the response from a hydrologic perspective.

The differences in the magnitude and spatial expression of southern Africa precipitation anomalies between the four ENSO and SIOD phase combinations during DJFM identified by Hoell et al. (2016) imply important shocks to the land surface hydrology of the region. The land surface hydrology of southern Africa is understudied in comparison with other areas of the world (Li et al. 2013), though several recommendations have been made on how to advance the expertise and tools necessary to improve that understanding (Hughes et al. 2015). Few studies, like Li et al. (2013), have focused on the regionwide land surface hydrology of southern Africa during the approximate 6-month wet and dry seasons. Other studies focus primarily on major river basins, such as the Zambezi, since these river basins are relied upon for hydroelectric power generation and water consumption (e.g., Vörösmarty and Moore 1991; Beck and Bernauer 2011). However, there lacks specific focus on how precipitation inputs to the land surface hydrology occur as a result of the combined effects of ENSO and SIOD, and these connections have important implications for local land-use decisions in conservation-focused regions such as TFCAs and regional management initiatives undertaken by organizations such as the Kavango–Zambezi Transfrontier Conservation Secretariat (KAZA TFCA 2016).

Specifically, regional hydrologic patterns influenced by anomalous climate patterns will impact multifaceted linkages between physical landscapes, wildlife, and human well-being (Schulze 2000; Hartter et al. 2012). These linkages are even more susceptible within TFCAs, large ecological regions that are bound by collaborative management and shared natural and cultural resources (SADC 2016). Better understanding of precipitation variability is important for improved natural resource management and local-scale agricultural efforts (Snyman 1998). Cooperatives that exist across these transboundary regions often rely on an adaptive management framework to address issues such as human–wildlife conflict, shared natural resource use, and land-use designations (SADC 2016). How underlying climate forcings may influence increased or decreased amounts of rainfall or contribute to the duration or magnitude of rains for a given year is valuable information for policy-makers and farmers alike in deciding what crops to plant, the timing of planting, and how to best manage local resources for both livestock and wildlife (Gaughan and Waylen 2012).

TABLE 1. Summary of meteorological datasets used to construct the Sheffield et al. (2006) forcing. See also Table 1 in Sheffield et al. (2006) for additional information.

Dataset	Variables
NCEP–NCAR Reanalysis I (Kalnay et al. 1996)	Precipitation
	Surface air temperature
	Downward shortwave radiation
	Downward longwave radiation
	Specific humidity
	Surface air pressure
	Wind speed
CRU TS2.0 (Mitchell and Jones 2005)	Precipitation
	Surface air temperature
	Cloud cover
GPCP (Huffman et al. 2001)	Precipitation
TRMM (Huffman et al. 2003)	Precipitation
NASA Langley SRB (Stackhouse et al. 2004)	Downward shortwave radiation
	Downward longwave radiation

Southern Africa has 18 potential or existing TFCAs that cover both terrestrial and marine environments (SADC 2016). Three well-established TFCAs, representing different parts of southern Africa, are used as reference points to illustrate the influence on land surface hydrology patterns due to the combined underlying forcings of ENSO and SIOD phases. All three TFCAs identify water resource, climate variability, and climate change as main challenges in sustainable, long-term management of the areas (SADC 2016). In this paper, we use simulations from a large-scale hydrologic model to examine the synchronous effects of El Niño, La Niña, and SIOD phasing on the land surface hydrology of southern Africa during 1950–2012. The land surface hydrology is represented by simulations of evapotranspiration, runoff, and soil moisture in addition to the model inputs of precipitation and 2-m air temperature. In section 2, we describe the methodology and hydrologic model. In section 3, we describe the simulated effects of ENSO and SIOD on southern Africa land surface hydrology, in terms of spatial features during DJFM and the temporal evolution over key TFCAs. In section 4, we provide a summary and discuss the significance of this work.

2. Models and methods

a. Study region

We focus on southern Africa, defined hereafter as the African continent south of 15°S, and emphasize three established TFCAs characterized by different climatic drivers and varying amounts of mean annual rainfall.

TABLE 2. DJFM 1950–2012 ENSO and SIOD occurrences.

	El Niño (18)	La Niña (21)
+SIOD (21)	1965/66, 1968/69, 1976/77, 1986/87, 1987/88, 2004/05, 2006/07 (7)	1950/51, 1954/55, 1967/68, 1970/71, 1973/74, 1975/76, 1985/86, 1988/89, 1998/99, 2000/01, 2005/06, 2007/08, 2008/09, 2010/11 (14)
−SIOD (19)	1957/58, 1963/64, 1969/70, 1972/73, 1977/78, 1982/83, 1991/92, 1994/95, 1997/98, 2002/03, 2009/10 (11)	1955/56, 1967/68, 1983/84, 1984/85, 1995/96, 1999/2000, 2011/12 (7)

Knowledge of climate patterns and variability in precipitation are becoming more prominent in management initiatives for communal farm-level practices and also conservation-based land decisions (Chishakwe et al. 2012). In addition, there is an increasing emphasis on shifting these management initiatives from a local-level focus to an integrated multilevel approach that also incorporates a regional, landscape-level perspective (Opdam and Wascher 2004). This idea conforms to the underlying rationale for TFCA formations that place explicit emphasis on the regional-scale ecohydrologic functioning of a system. Thus, an explicit focus on how results from this study influence the ecohydrologic functioning of the different TFCAs provides a framework from which conservation and land managers can start to shape policy decisions regarding climate patterns.

In the north-central part of southern Africa is the Kavango–Zambezi Conservation Area (KAZA), which has an area of 440 000 km^2 and is considered the largest internationally managed terrestrial conservation area in the world (Cumming 2008). The multifunctional landscape of KAZA includes multiple protected areas interspersed with communal lands and includes parts of Namibia, Botswana, Angola, Zambia, and Zimbabwe. Hydroclimatologically, the KAZA region cuts across three catchments in southern Africa: Okavango, Kwando, and Zambezi, all of which, at times, are interconnected, but each represents transboundary, perennial water sources that are important for both wildlife and people. The climate of KAZA is controlled primarily by the ITCZ, and therefore the total mean annual rainfall of 400–1000 mm (Cumming 2008) is largely a result of local convection. In the southeastern part of southern Africa is the Greater Limpopo Transfrontier Park (GLTP), which includes parts of Mozambique, Zimbabwe, and South Africa and covers a total area of 99 800 km^2 (Wolmer 2003). The TFCA includes national parks in each country as well as a mixture of communal and private areas and

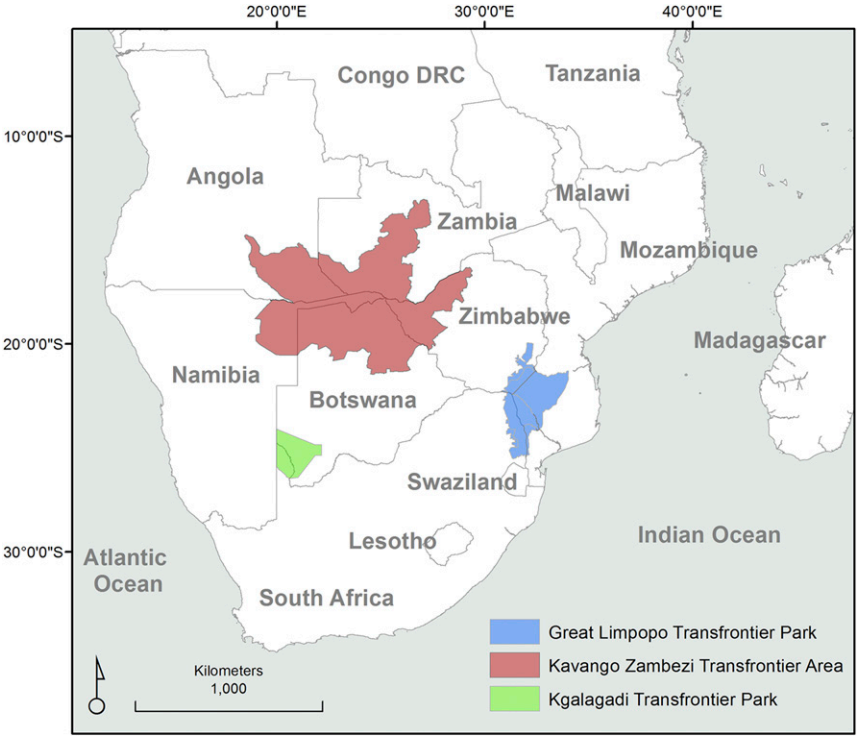

FIG. 1. Study region with focus areas outlined in color.

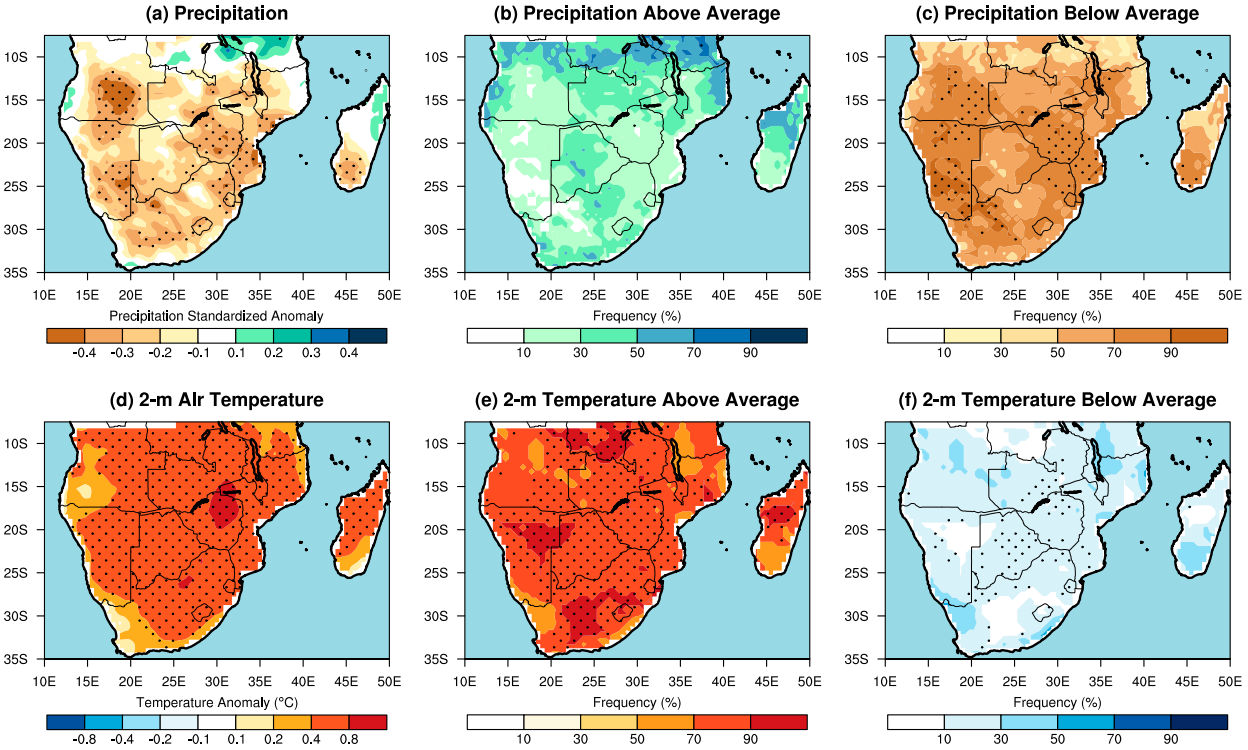

FIG. 2. DJFM 1950–2012 EN-SIOD composites of (a) standardized precipitation anomaly, (b) frequency of above-average precipitation (%), (c) frequency of below-average precipitation (%), (d) 2-m air temperature anomaly (°C), (e) frequency of above-average 2-m temperature (%), and (f) frequency of below-average 2-m temperature (%). Stippling denotes anomalies or frequencies significant at $p < 0.05$.

averages an annual rainfall of 530 mm. Because of its location within southern Africa, the precipitation of GLTP is governed by westward-moving mesoscale convective complexes and tropical cyclones. Third and smallest of the TFCAs is the Kgalagadi Transfrontier Park (KG), which is a TFCA including South Africa's Kalahari Gemsbok National Park and Bostwana's Gemsbok National Park (~35 500 km^2). The KG TFCA has the lowest mean annual rainfall at 220 mm and provides an example of a different extreme, being a landscape largely devoid of human presence and characterized largely by sparse vegetation and red Kalahari sands. The KG landscape is governed by a local heat low and cloud bands that spark the sparse regional rainfall. However, the area is a rich ecosystem with over 60 ungulate and other mammalian species, and knowledge about drought and flood events associated with underlying climate modes is a relevant strategy for successful management in the region (Opdam and Wascher 2004).

b. *Hydrologic model*

The time-varying land surface hydrology during 1950–2012 for this study comes from the Variable Infiltration Capacity (VIC) model (Liang et al. 1994, 1996) simulation initialized in 1948, as described in Nijssen et al. (2014). We discard the first two years of the simulation since land surface models take at least a few years to reach equilibrium, especially in terms of soil moisture in the deeper layers (Cosgrove et al. 2003). The VIC model is implemented at 0.5° × 0.5° and is forced by the observed time-varying meteorology. The VIC model is a widely used macroscale hydrologic model (e.g., Sheffield and Wood 2008; Livneh et al. 2013; Shukla et al. 2013. Among the primary features of the VIC model (Nijssen et al. 2001; Shukla et al. 2014) include its ability to allow for subgrid variability in land cover classes and the soil moisture storage capacity. Total actual evapotranspiration for each grid cell is calculated by first calculating transpiration and evaporation over canopy and/or bare soil for each land cover class within that grid and then by aggregating those values from each land cover class based on the respective fraction of the area covered. The soil profile is generally separated into three layers. Movement of moisture in the VIC model is allowed between the top two layers as well as the bottom two layers. Base flow in the VIC model is modeled nonlinearly based on the soil moisture of the bottom layer (Todini 1996). Vegetation, elevation, and soil parameters for this study were specified (Nijssen et al. 2001),

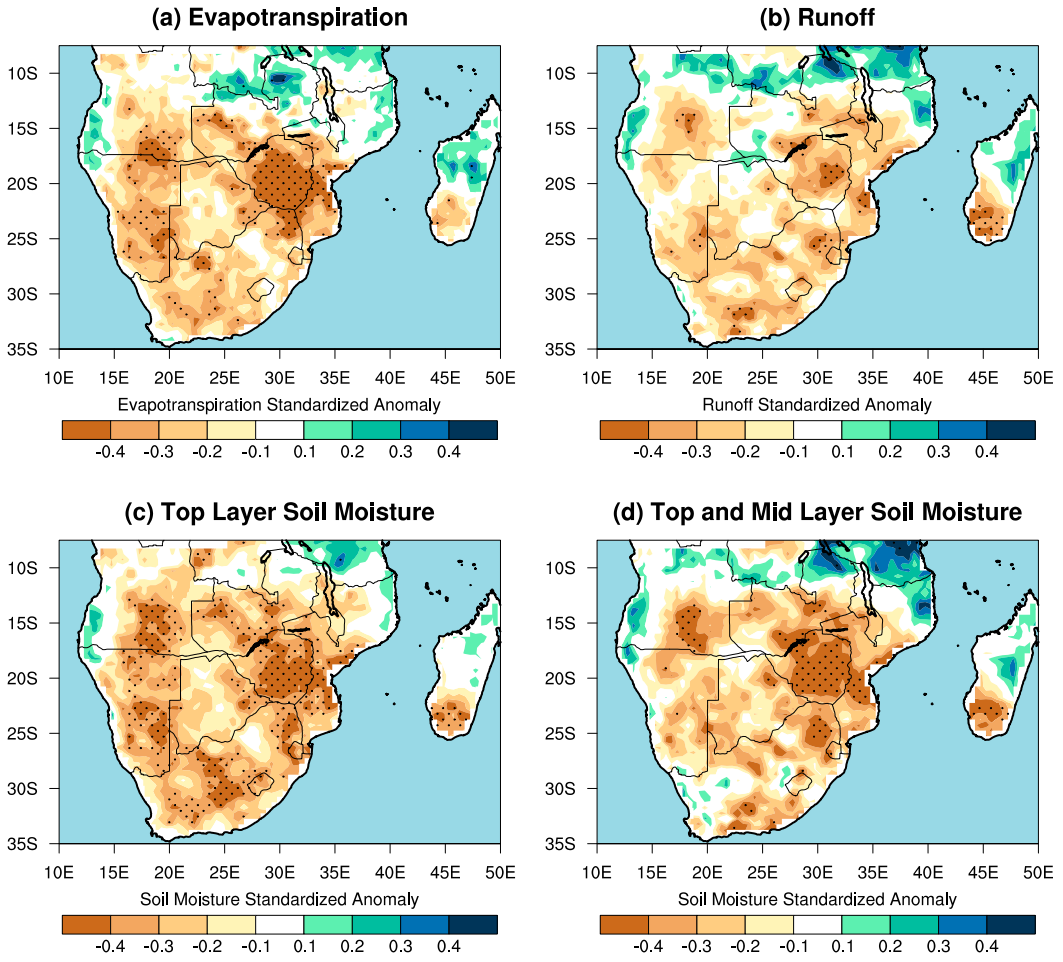

FIG. 3. DJFM 1950–2012 EN-SIOD standardized anomaly composites of (a) evapotranspiration, (b) runoff, (c) top-layer soil moisture, and (d) top- and midlayer soil moisture. Stippling denotes anomalies significant at $p < 0.05$.

and the model simulation was performed in water balance mode using a daily time step (Nijssen et al. 2014).

For this simulation, the VIC model was forced with daily meteorological variables: precipitation, maximum and minimum 2-m air temperature, and wind speed data from Sheffield et al. (2006). Sheffield et al. (2006) is a widely used global forcing dataset and currently supports real-time drought monitoring systems such as Princeton's Africa Flood and Drought Monitor (http://stream.princeton.edu/AWCM/WEBPAGE/interface.php?locale=en). At the core of this dataset is the National Centers for Environmental Prediction–National Center for Atmospheric Research (NCEP–NCAR) reanalysis that has been corrected for several of the known biases in the reanalysis datasets (e.g., mean climatological bias, rain day statistics, undercatch bias) using several global observations. The global datasets that have been used for different corrections of the Sheffield et al. (2006) forcing are summarized in Table 1. Further details on the atmospheric forcings, soil, elevation, and vegetation parameters specified in this VIC simulation can be found in Nijssen et al. (2014).

In this paper, the observed precipitation used to drive the VIC model is analyzed, in addition to the VIC simulations of daily average 2-m air temperature, evapotranspiration, runoff, top layer soil moisture (from the surface to 30 cm), and top and midlayer soil moisture (from the surface to ~400 cm). All variables are displayed as standardized anomalies relative to a 1950–2012 climatology, except 2-m air temperature that is displayed as an anomaly. Standardized anomalies provide a fair comparison among components of the water budget since the mean absolute value of water budget components differs considerably over regions such as southern Africa. Most of the precipitation input gets output in terms of evapotranspiration, and the value of runoff is much smaller than evapotranspiration.

Considering that the land surface hydrology of southern Africa is understudied in comparison with

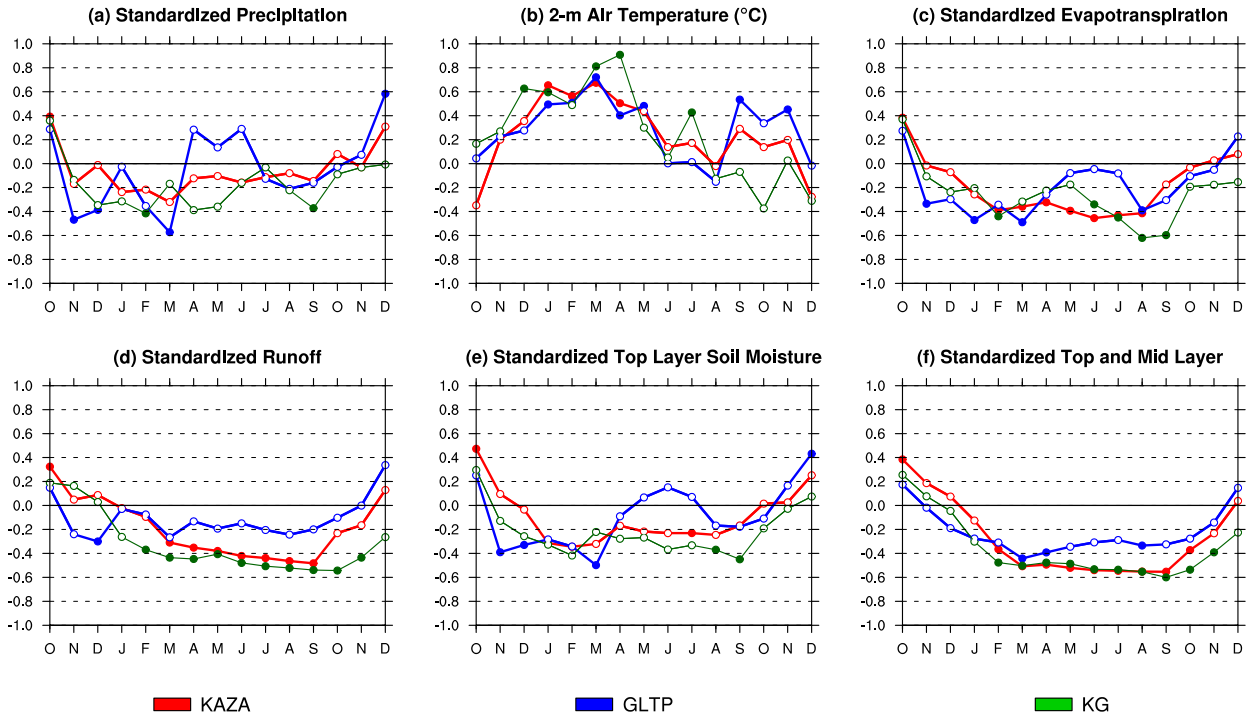

FIG. 4. Monthly composites before, during, and after EN-SIOD areally averaged over KAZA (red), GLTP (blue), and KG (green) displayed in terms of (a) standardized precipitation anomaly, (b) 2-m air temperature anomaly (°C), (c) standardized evapotranspiration anomaly, (d) standardized runoff anomaly, (e) standardized top-layer soil moisture anomaly, and (f) standardized top- and midlayer soil moisture anomaly. Closed circles denote anomalies significant at $p < 0.05$.

other areas of the world (Li et al. 2013), few studies have examined the hydrology of southern Africa with the VIC model. In one of the earliest studies, Nijssen et al. (2001) estimated a seasonal climatology of hydrologic variables globally in terms of soil moisture, evapotranspiration, and soil water equivalent. Examples of examinations of Africa that utilized the VIC model include Marshall et al. (2012) and Guan et al. (2014). Marshall et al. (2012) used VIC simulations to evaluate evapotranspiration trends in Africa, noting that the VIC model captured characteristics of runoff better than other land surface models, while Guan et al. (2014) used VIC simulations of soil moisture to supplement their analysis on the land surface phenology of African savannahs and woodlands.

c. *Methods*

1) DEFINITION OF ENSO AND SIOD PHASE COMBINATIONS

Four ENSO and SIOD phase combinations are identified for the DJFM season during 1950–2012: El Niño and negative SIOD (EN-SIOD), El Niño and positive SIOD (EN+SIOD), La Niña and negative SIOD (LN-SIOD), and La Niña and positive SIOD (LN+SIOD). The DJFM occurrences of the four ENSO and SIOD phase combinations are shown in Table 2. The ENSO and SIOD phase combinations are defined for DJFM since the ENSO and southern Africa precipitation coupling is strongest during this 4-month season (Manatsa et al. 2015). El Niño and La Niña events are identified using a threshold exceedance of the DJFM average Niño-3.4 index anomaly, where the Niño-3.4 index is defined as the areally averaged SST over 5°S–5°N, 170°–120°W. El Niño events are defined when the Niño-3.4 index exceeds 0.5°C, and La Niña events are defined when the Niño-3.4 index falls below −0.5°C. The DJFM average sign of the SIOD anomaly is identified using the SIOD index of Behera and Yamagata (2001), which is defined as the areally averaged SST anomaly over 28°S–18°N, 90°–100°E subtracted from the areally averaged SST over 37°–27°S, 55°–65°E. The Niño-3.4 and SIOD anomaly indices are calculated from the merged Hadley–NOAA/OISST dataset developed by Hurrell et al. (2008) using a 1950–2012 climatology.

2) SIGNIFICANCE TESTING

The statistical significance of land surface anomalies associated with ENSO and SIOD phase combinations at each grid point during DJFM and areal averages of

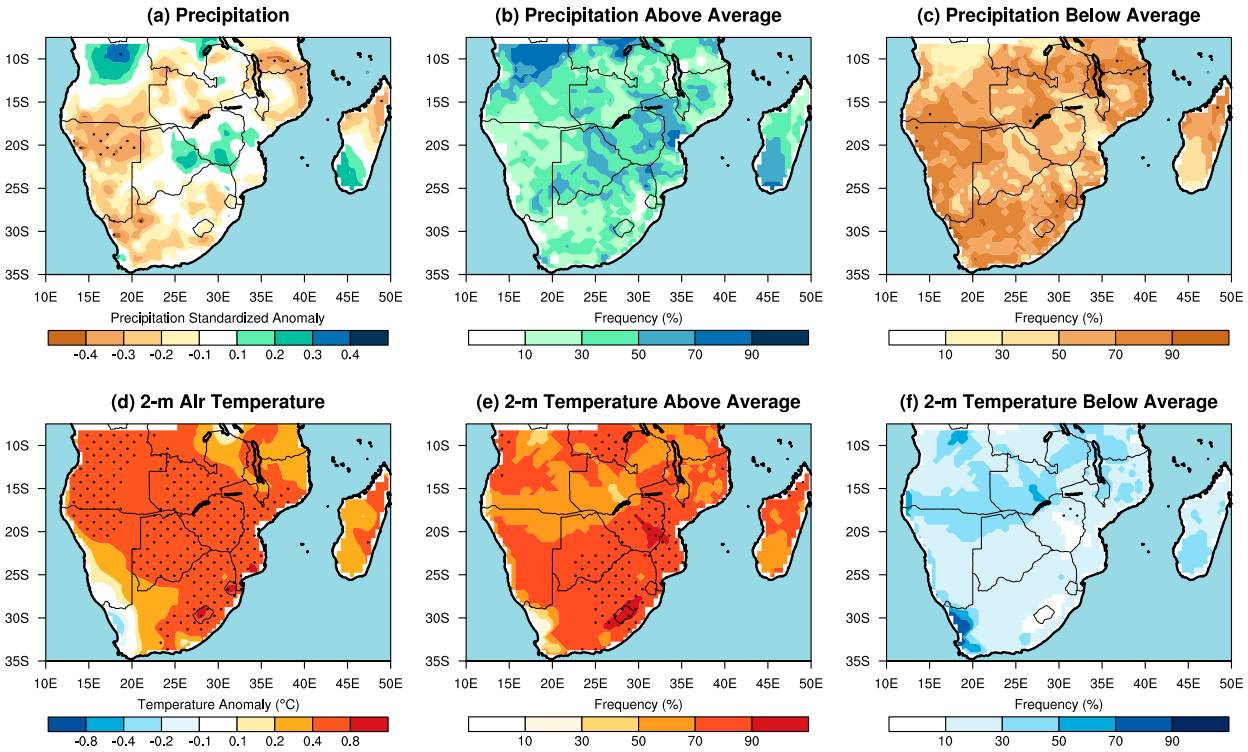

FIG. 5. As in Fig. 2, but for EN+SIOD.

monthly regional conditions are assessed through a resampling approach. A random sample of each variable, whose size corresponds to the number of occurrences of each ENSO and SIOD phase combination, is selected without replacement from the 1950–2012 time series. The random samples are averaged, and the process is repeated 10 000 times to construct a distribution. The statistical significance at $p < 0.05$ ($p < 0.025$ at each tail) is assessed from this distribution. For example, to assess the statistical significance of the EN-SIOD phase combination, 11 samples are drawn without replacement from the 1950–2012 time series. The 11 samples are averaged and the process is repeated 10 000 times. The statistical significance thresholds at $p < 0.05$ are identified from the 9500th and 500th values of the sorted 10 000-member distribution.

3. ENSO/SIOD relationships with southern Africa land surface hydrology

The land surface hydrology associated with the four ENSO and SIOD phase combinations shown in Table 2 are examined similarly. First, the contemporaneous spatial relationships between the ENSO and SIOD phase combinations during DJFM 1950–2012 are evaluated. This analysis is carried out through an examination of precipitation and 2-m air temperature, in terms of average standardized anomalies and the frequency of occurrence of above- or below-average anomalies during DJFM periods that meet the ENSO and SIOD phase criteria. The spatial evapotranspiration, runoff, and soil moisture at various depths are similarly evaluated. Finally, the lasting temporal effects of ENSO–SIOD phase combinations are evaluated over the three TFCAs (Fig. 1). To identify the regional effects over each TFCA, we examine the average monthly anomalies areally averaged over each region prior to, during, and after the ENSO and SIOD phase criteria is met for DJFM. These lasting effects are examined in terms of evapotranspiration, runoff, and two soil moisture depth profiles.

a. *EN-SIOD*

The EN-SIOD phasing is linked with widespread dryness over southern Africa during DJFM, but with important regional variations in the magnitude of significance patterns of the precipitation anomalies (Figs. 2a–c). Statistically significant drying is found to occur primarily in coastal countries of southern Africa. Other countries such as Botswana and Zambia are also found to be dry, though the drying is not statistically significant. EN-SIOD is also related with a north-to-south wet–dry dipole over Madagascar, of which only the drying is statistically significant. This anomalous

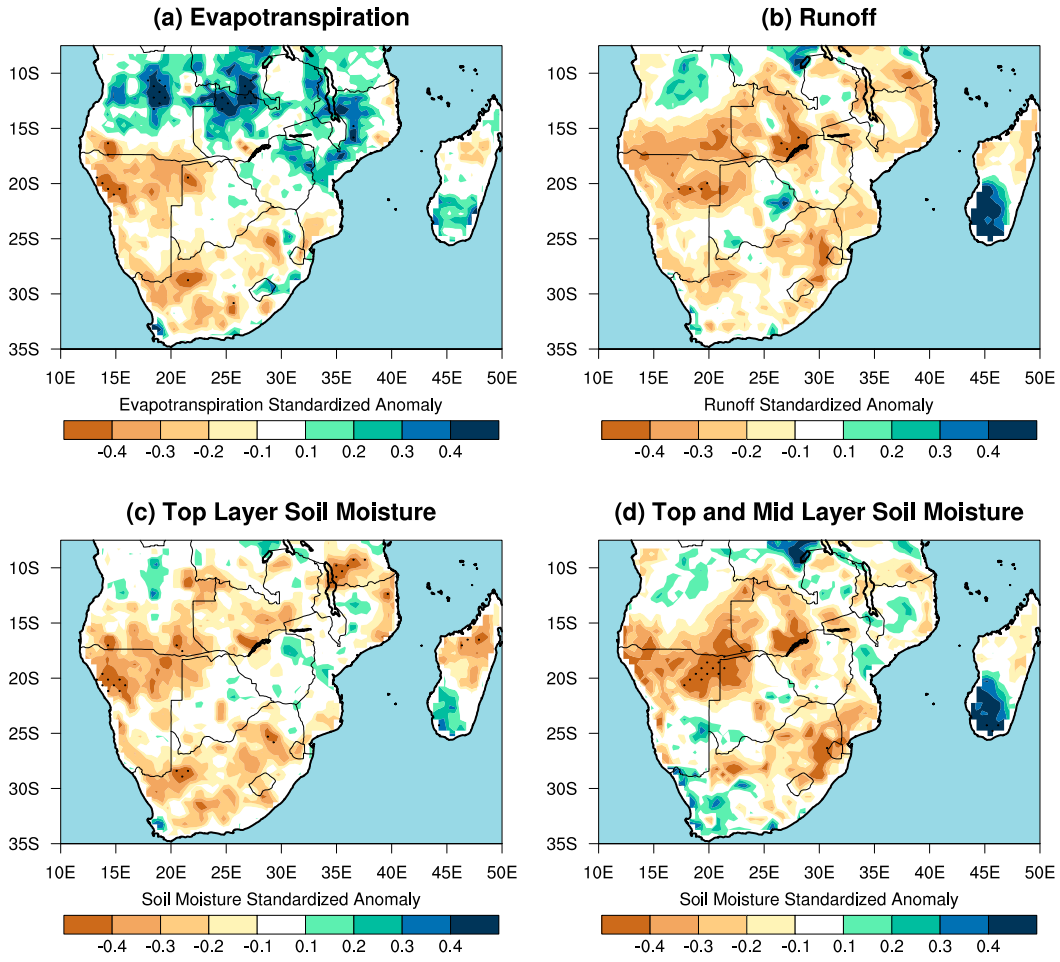

FIG. 6. As in Fig. 3, but for EN+SIOD.

precipitation pattern over Madagascar is related with the preferred tracks of landfalling tropical cyclones during the EN-SIOD phasing (Ash and Matyas 2012). The anomalous dry DJFM conditions are associated with statistically significant increases in the frequency of dry seasons during the EN-SIOD phasing.

The EN-SIOD phasing is also linked with widespread warm anomalies in 2-m air temperature over southern Africa during DJFM (Figs. 2e,f). Significant warm anomalies in 2-m air temperature cover the entire region, except for a small portion of northwestern Namibia, coastal Angola, and southern Madagascar. The warmest 2-m air temperature anomalies are primarily confined away from the Atlantic and Indian coastlines, typified by the largest magnitudes over the lowlands of the Okavango and Orange River basins. The anomalously warm DJFM 2-m air temperatures across the region are associated with significant increases in the frequency of warm seasons during the EN-SIOD phasing. Additionally, there is a significant decrease in the number of DJFM seasons in which 2-m air temperature is below average over Zambia, Zimbabwe, and Botswana during the EN-SIOD phasing.

The significant widespread decreases in precipitation and increases in 2-m air temperature during DJFM of EN-SIOD years lead to important contemporaneous hydrologic effects over southern Africa (Fig. 3). The magnitude and pattern of significant evapotranspiration anomalies and top-layer soil moisture anomalies closely follows the contemporaneous precipitation anomalies, notably with the largest decreases over Mozambique and Zimbabwe in the east and over Namibia and southern Angola to the west. The top- and middle-layer soil moisture effects are not nearly as widespread as the other hydrologic variables, as significant widespread anomalies are only found over southern Mozambique and Zimbabwe during EN-SIOD. Runoff is generally reduced regionwide during EN-SIOD and follows a fairly similar pattern with the contemporaneous precipitation anomalies, but the anomalies shown to be significant are quite sparse.

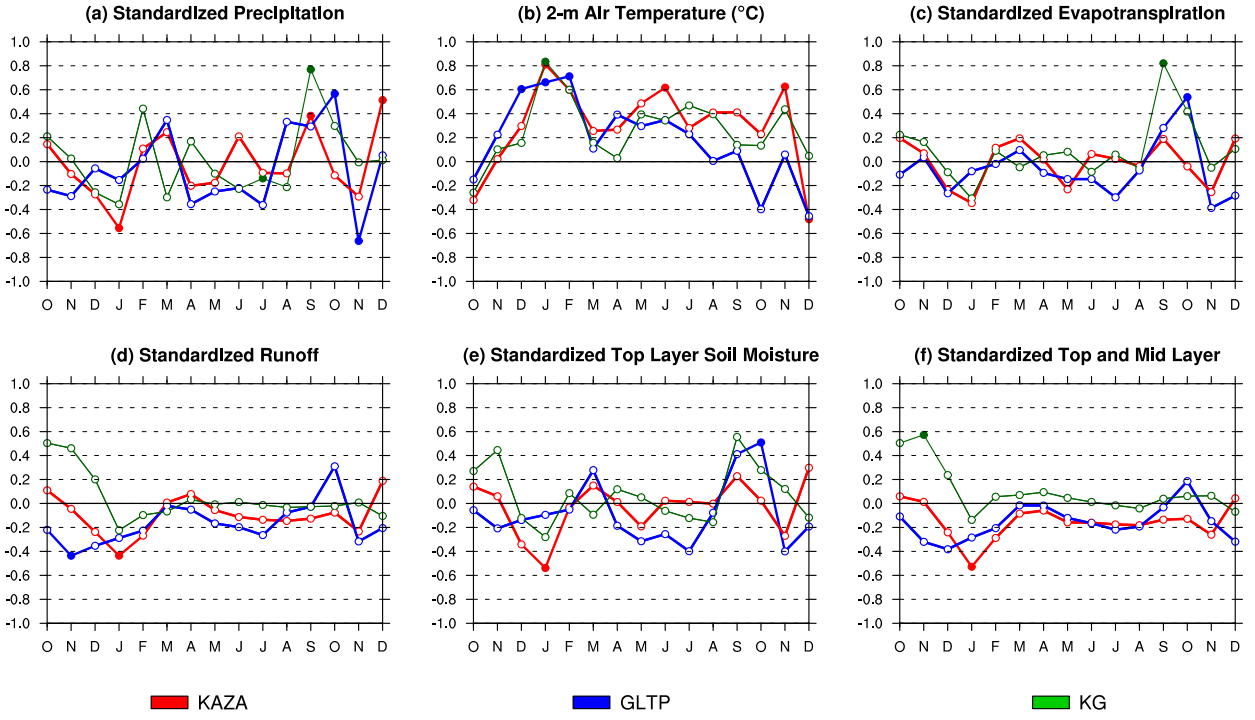

FIG. 7. As in Fig. 4, but for EN+SIOD.

The significant regional precipitation and 2-m air temperature anomalies associated with EN-SIOD are primarily confined to the DJFM season for each TFCA (Figs. 4a,b), though warm 2-m air temperature anomalies do persist into April and May and are associated with negative evapotranspiration anomalies. The lasting effects on the regional hydrology over the KAZA, GLTP, and KG basins (Figs. 4c–f) are therefore primarily a result of the regionwide changes in precipitation and temperature during DJFM of the EN-SIOD years (Fig. 2).

The lasting hydrologic effects of EN-SIOD are most strongly felt over KAZA (Figs. 4c–f), where both hydrologic drought, measured in terms of significant runoff departures (Fig. 4c), and agricultural drought, measured in terms of significant evapotranspiration departures (Fig. 4d), remain until nearly the beginning of the following rainy season. Reductions in evapotranspiration and runoff indicate negative effects upon vegetation health and water availability, respectively. While top-layer soil moisture over KAZA recovers quickly after DJFM of the EN-SIOD season (Fig. 4e), the soil moisture within the top and middle layers remains below average until December of the following rainy season (Fig. 4f).

By contrast, the hydrologic effects of EN-SIOD are not nearly as strongly felt over GLTP and KG as they are over KAZA (Figs. 4c–f). For KG, runoff remains significantly below average until the July following EN-SIOD, and top- and middle-layer soil moisture remains below average until the advent of the following rainy season. For GLTP, evapotranspiration, runoff, and soil moisture at all levels recover within the first few months after the DJFM rainy season of EN-SIOD.

b. *EN+SIOD*

The EN+SIOD phasing is unrelated to statistically significant precipitation anomalies over southern Africa during DJFM (Figs. 5a–c). There are, however, two important precipitation features associated with EN+SIOD. First, EN+SIOD increases precipitation over KAZA and KG. Second, EN+SIOD is related to a north-to-south dry–wet dipole over Madagascar and related drying across the Mozambique Channel and over northern Mozambique and southern Tanzania. These precipitation anomalies are related to a change in the track of tropical storms entering the region, an increased frequency of storms over southern Madagascar, and a decreased frequency of storms over northern Madagascar and northern Mozambique modulated by the EN+SIOD phasing (Ash and Matyas 2012). The lack of significant precipitation anomalies throughout the region are related to insignificant changes in the number of DJFM seasons in which precipitation was either above or below average when the EN+SIOD criterion was met (Figs. 5b,c).

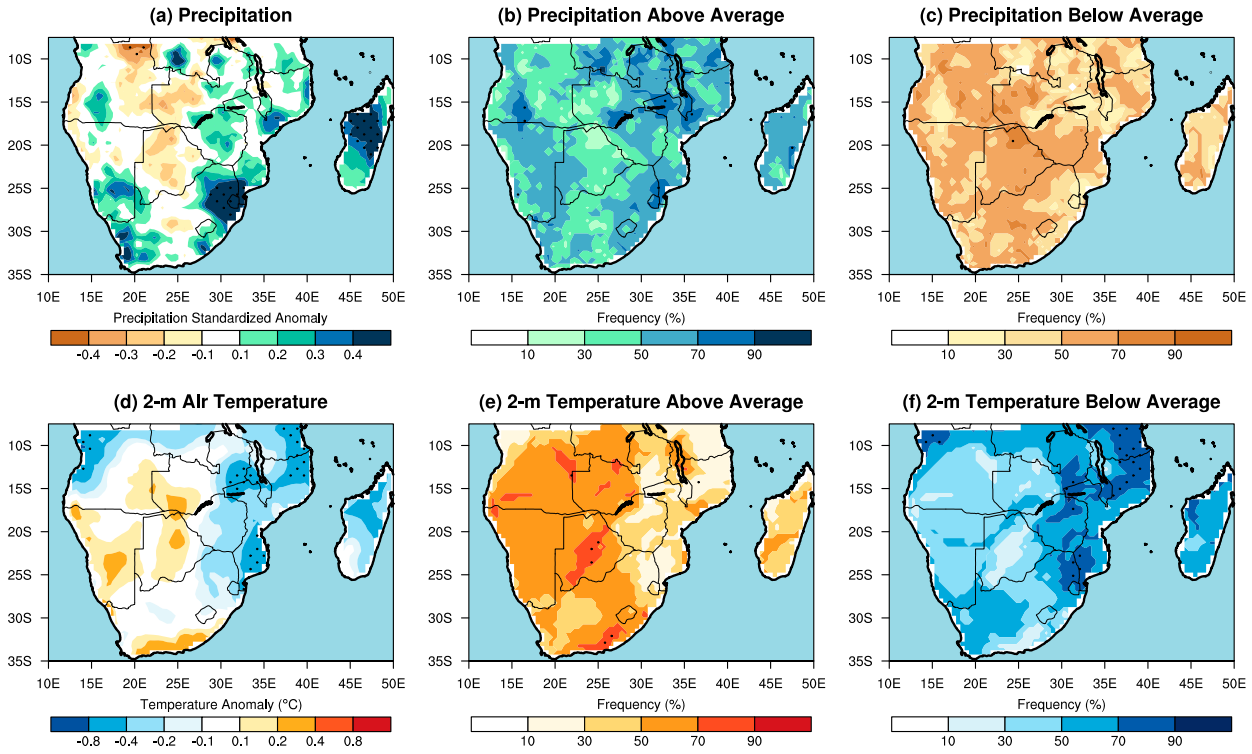

FIG. 8. As in Fig. 2, but for LN-SIOD.

The EN+SIOD phasing is linked with warm anomalies in 2-m air temperature over southern Africa during DJFM, though not as widespread or as strong in magnitude as during the EN-SIOD phasing (cf. Figs 4e,f and 5e,f). Significant warm anomalies are found primarily along a northwest to southeast axis, extending from Angola to South Africa, with only an area of southeast Angola devoid of such significant anomalies. The warmest anomalies, on the order of 0.5°C, are located over southeastern portions of southern Africa, including the GTLP region. The anomalously warm DJFM 2-m air temperatures across southeastern southern Africa are largely a result of statistically significant increases in the frequency of warm seasons during the EN+SIOD phasing. However, there are no significant decreases in the number of DJFM seasons in which 2-m air temperature is below average regionwide.

EN+SIOD during DJFM does not show the same type of widespread significant contemporaneous and long-lasting hydrologic effects over southern Africa and the three Transfrontier Park focus regions as does the EN-SIOD coupling (Figs. 6, 7). The lack of important significant hydrologic effects comes as little surprise since EN+SIOD is unrelated to significant departures in precipitation throughout the entire region (Fig. 5). One exception to this, however, is during January of EN+SIOD years, where the composites show a significant decrease in precipitation over KAZA, which corresponds with significant January decreases in evapotranspiration, runoff, and soil moisture (Fig. 7).

c. *LN-SIOD*

The LN-SIOD phasing has a spatially inconsistent pattern of precipitation anomalies across southern Africa during DJFM (Figs. 8a–c). The LN-SIOD phasing is linked with wet anomalies along Atlantic and Pacific coastlines of southern Africa and dry anomalies over the interior of the region, spanning the countries of Botswana, Zimbabwe, and Angola. DJFM precipitation anomalies across the region are weak, as the only areas of significant precipitation anomalies are confined to the wet regions of northeastern southern Africa, from central to northern Mozambique and northern Madagascar. The regionwide statistically insignificant precipitation anomalies are largely a result of equal occurrences of above- and below-average precipitation across the LN-SIOD events (Figs. 8b,c).

The 2-m air temperature anomaly pattern over southern Africa during LN-SIOD is also spatially inconsistent and closely matches the precipitation anomaly pattern (Fig. 8), which implies a tight coupling between the regional temperature and precipitation

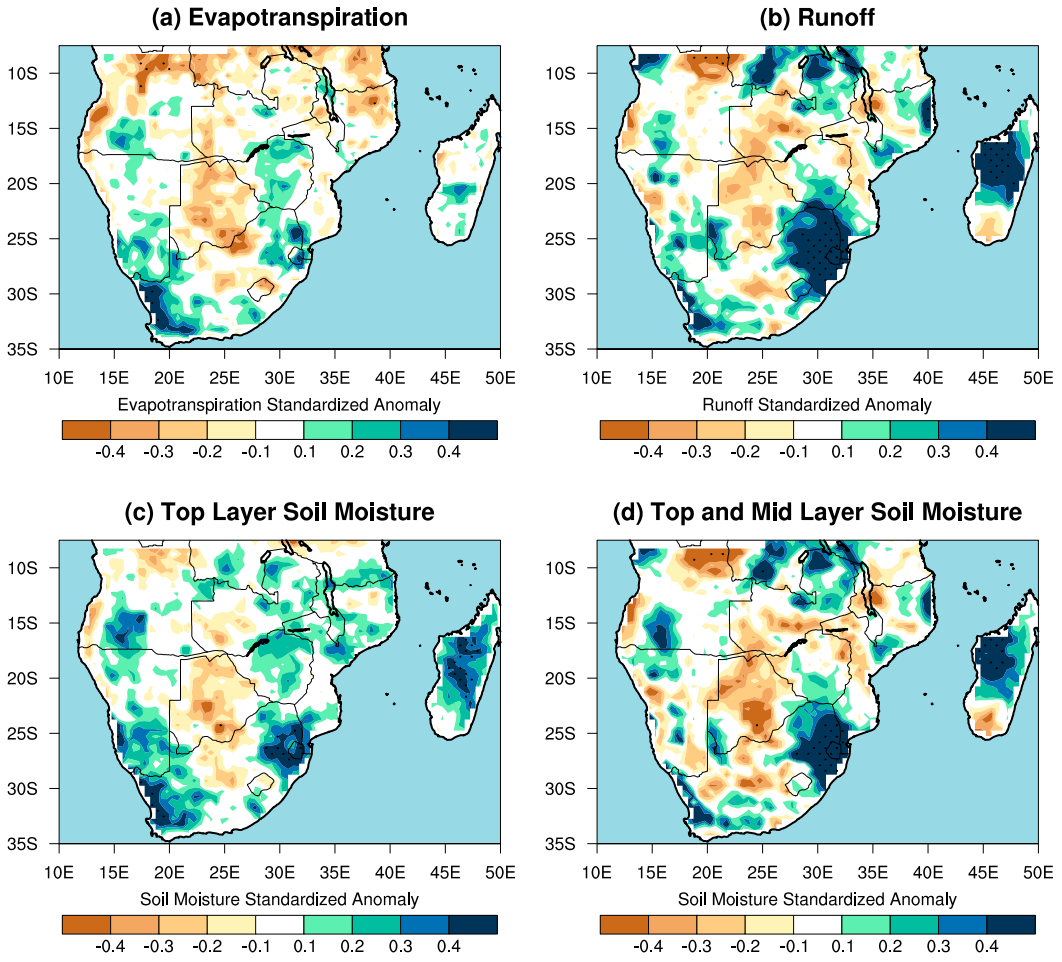

FIG. 9. As in Fig. 3, but for LN-SIOD.

during LN-SIOD. Cool anomalies are largely found over areas of above-average precipitation and warm anomalies are largely found over areas of below-average precipitation (Fig. 8d). Similar to the precipitation anomalies during LN-SIOD (Fig. 8a), the only area of significant 2-m air temperature anomalies are the cool temperature anomalies along coastal areas of the Mozambique Channel (Fig. 8d). The statistically significant areas of cool temperature anomalies are associated with a significant increase in the frequency of DJFM seasons of below average 2-m air temperature (Fig. 8f).

Changes in the hydrologic variables associated with LN-SIOD during DJFM closely correspond with the changes in precipitation and temperature (Fig. 9). Areas that experience above-average precipitation and below-average 2-m air temperature experience higher runoff, evapotranspiration, and soil moisture while areas that experience below-average precipitation and above-average 2-m air temperature experience lower runoff, evapotranspiration, and soil moisture. There is a general lack of statistically significant changes in the hydrologic variables across southern Africa during DJFM associated with LN-SIOD, with the exception of runoff and soil moisture over northeastern South Africa and southern Mozambique. Over our three Transfrontier Park focus regions, the rather weak changes in temperature and precipitation during DJFM of LN-SIOD do not translate to long-lived anomalies in the hydrologic variables (Fig. 10).

d. LN+SIOD

The LN+SIOD phasing is linked with widespread above-average precipitation anomalies over southern Africa during DJFM (Figs. 11a–c). The widespread above-average anomalies are strongest and statistically significant over the western sector of the region, across Angola, Namibia, Botswana, and southwestern South Africa. By contrast, LN+SIOD is related to near-average precipitation throughout areas adjacent to the Mozambique Channel and across Madagascar. The

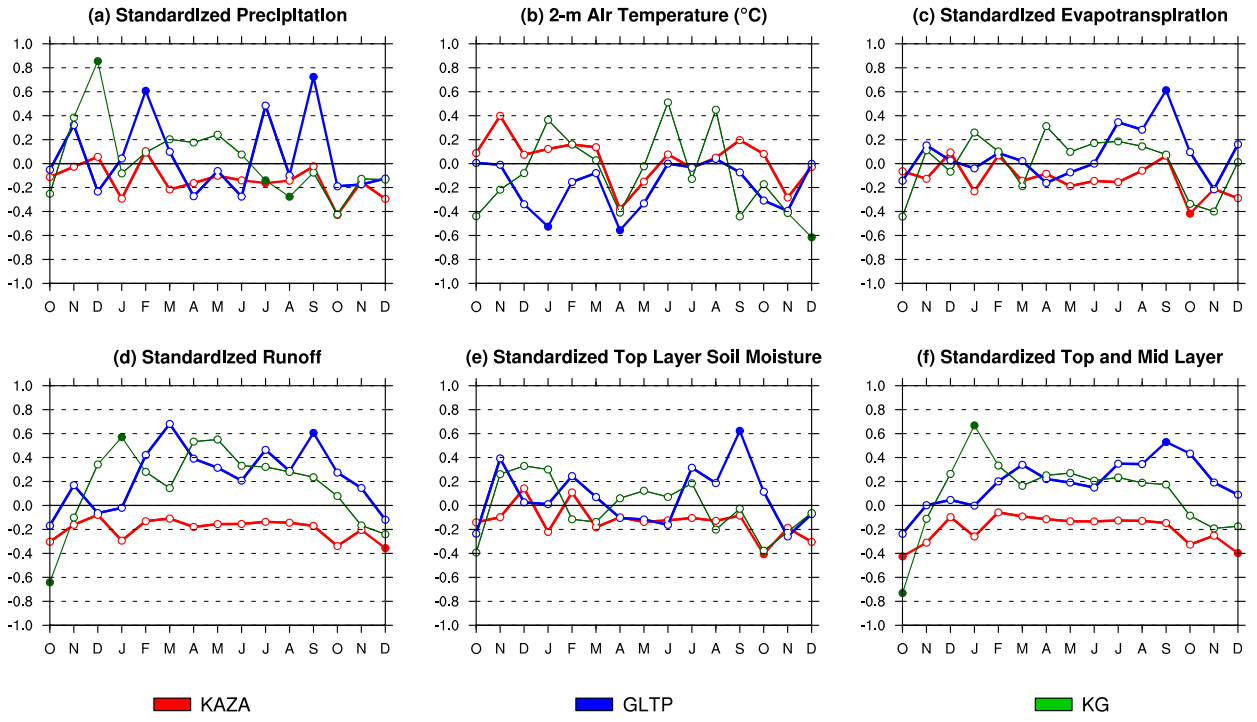

FIG. 10. As in Fig. 4, but for LN-SIOD.

above-average precipitation anomalies over the western sector of southern Africa during LN+SIOD are related to significant increases in the frequency of above-average precipitation and decreases in the frequency of below-average precipitation (Figs. 11b,c).

The LN+SIOD phasing is also linked with contemporaneous widespread cold anomalies in 2-m air temperature throughout southern Africa during DJFM (Figs. 11e,f). Significant cold anomalies in 2-m air temperature cover the entire region, except for areas within about 200 km of all coastlines. The anomalously cool DJFM 2-m air temperatures regionwide are a result of significant increases in the frequency of cool seasons and significant decreases in the frequency of warm seasons during the LN+SIOD phasing.

The changes in precipitation during LN+SIOD are related to contemporaneous DJFM changes in the hydrologic variables throughout southern Africa (Fig. 12). The entire western sector of southern Africa, west of Zimbabwe and northeastern South Africa, experiences above-average evapotranspiration, runoff, and soil moisture. Two of the three Transfrontier Park focus areas, KAZA and KG, fall within the region of strong DJFM precipitation increases and instantaneous changes in hydrologic variables. As such, the strong perturbations of the hydrologic variables persist; significant anomalies of evapotranspiration and top-level soil moisture last through the following winter while significant anomalies of runoff and top- and middle-layer soil moisture last into the beginning of the following summertime rainy season. However, since GLTP resides in a region in which LN+SIOD is not linked with strong DJFM precipitation anomalies, for example, the intersection of South Africa, Mozambique, and Zimbabwe, there are no significant instantaneous and long-lived changes in hydrologic variables.

4. Summary and discussion

Our study examines the instantaneous and long-lived relationships between the southern Africa land surface hydrology and ENSO and SIOD phasing during DJFM, the height of the region's rainy season. As ENSO and SIOD are primary controls of southern Africa climate during austral summer, this analysis offers information on the land surface hydrology during the year following an ENSO event, which will better inform managers and practitioners on the behavior of critical sources of water for both humans and wildlife across the region's various landscapes.

The subregional southern Africa precipitation (Figs. 2a, 5a, 8a, 11a) and temperature responses (Figs. 2d, 5d, 8d, 11d) to the four ENSO and SIOD phase combinations show that the response to ENSO and SIOD is not linear. This discovery provides

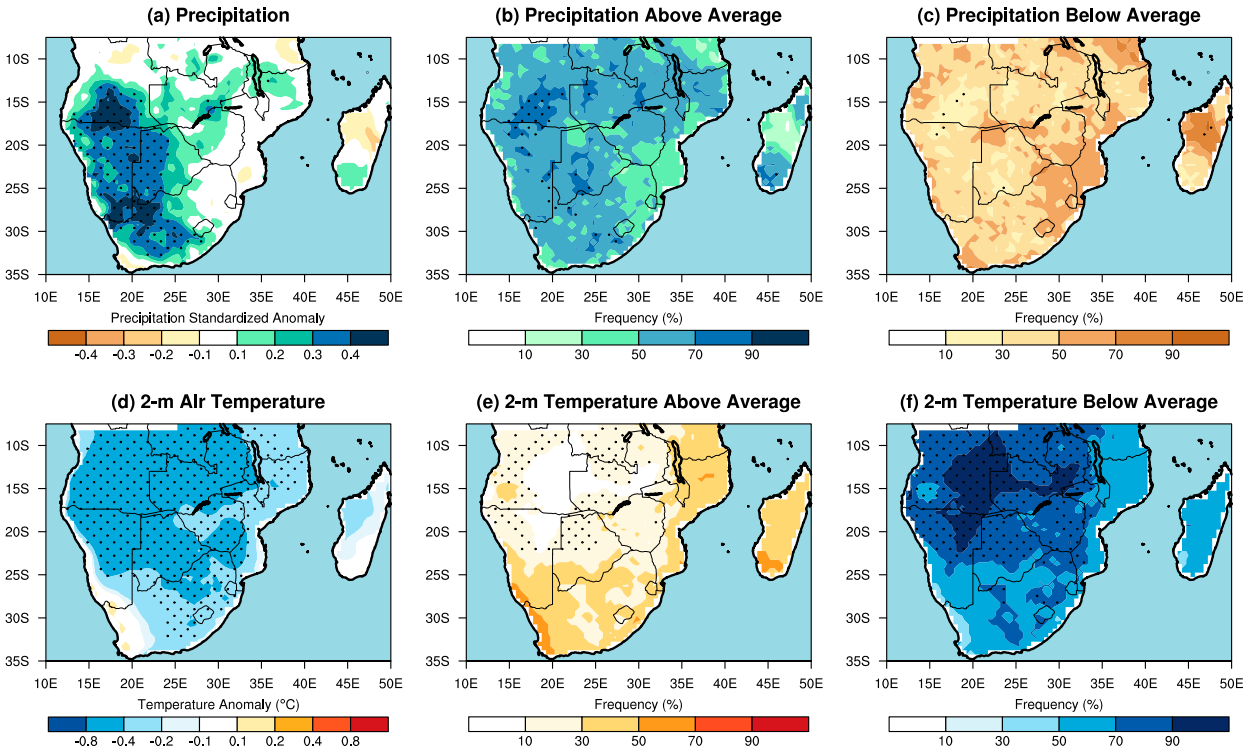

FIG. 11. As in Fig. 2, but for LN+SIOD.

valuable contexts to seasonal forecasters who have information on the forecast ENSO and SIOD state prior to the DJFM rainy season. Furthermore, our hydrologic analyses identify subregional variations related with ENSO and SIOD as well as the important synergies of temperature and precipitation in producing hydrologic anomalies that are relevant toward independent decision-making processes for the various TFCA across southern Africa.

Our results suggest that the synchronous ENSO and SIOD phasing has profound effects on the DJFM precipitation and temperature patterns across southern Africa and therefore the land surface hydrology throughout the following year into the next rainy season. We identified four ENSO and SIOD phase combinations during 1950–2012 and examined the land surface hydrology from those event classifications using variables extracted from one long-term simulation of the VIC model forced by the observed time-varying meteorology. When ENSO and SIOD are in opposing phases (e.g., EN-SIOD and LN+SIOD), regionwide precipitation anomalies occur. However, when ENSO and SIOD are in the same phase (e.g., EN+SIOD and LN-SIOD), weak and insignificant precipitation anomalies occur on average, which results in little effect on the land surface hydrology of the given TFCAs. While EN-SIOD and LN+SIOD phase combinations are by far the most impactful on the instantaneous and long-lived southern Africa land surface hydrology, they are not mirror images of one another. These differences indicate important nonlinearities that practitioners must be aware of when considering seasonal forecasts in the context of water resource management. For example, EN-SIOD is related to exceptionally dry conditions throughout nearly the entirety of southern Africa during DJFM. The subsequent effects of these conditions across the three TFCAs in the year following the event may manifest in important water availability implications for crop productivity, wildlife movements, and subsequent human nourishment. By contrast, LN+SIOD is related to exceptionally wet conditions across Angola, Namibia, Botswana, and southwestern South Africa and near-neutral conditions elsewhere.

Our study also suggests that the spatial patterns of ENSO and SIOD influence the TFCAs of southern Africa differently with varying implications for management. While all three TFCAs in this study are impacted by below-average precipitation and above-average temperature anomalies during EN-SIOD phases (Fig. 2), the GTLP has the most statistically significant influence due to these anomalous conditions (Fig. 4). However, the top- and midlayer soil moisture for all three TFCAs show a significant negative anomaly

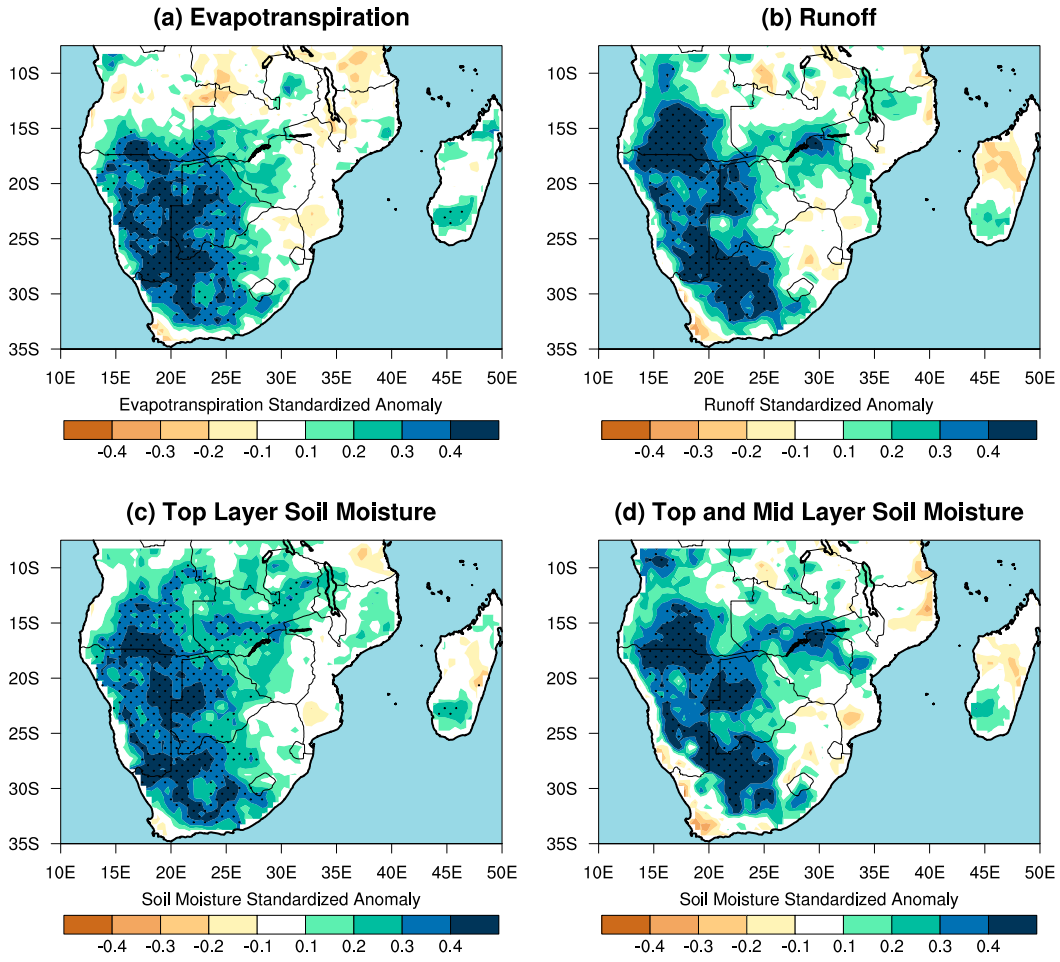

FIG. 12. As in Fig. 3, but for LN+SIOD.

during the months of March and April. This is important for both natural resource managers and farmers, as these are the months leading into the dry season and coincide with timing of harvest for rain-fed agricultural systems across the region. Drier soil conditions may contribute to the propensity of increased fires across the landscape and fewer seasonal watering holes, both of which will increase pressures with human–wildlife interactions (Tinley 1982). And while not as statistically significant, similar dry and warm conditions during EN+SIOD should also be recognized, even if the land surface hydrologic effects are not as impactful.

Similar to EN+SIOD, LN-SIOD phases do not have statistically significant associations across any of the three TFCAs, although patterns of anomalous precipitation are drier in KAZA versus wetter in the GTLP and KG regions more to the south. This results in increased soil moisture and runoff for the more southern TFCAs, which is even more pronounced during LN+SIOD phases (Fig. 13). It is important to note, however, that the Transfrontier Conservation Areas affected by positive anomalous runoff and soil moisture patterns during LN+SIOD phases switch to the two more western TFCAs, KAZA and KG, with less strength of association for the GTLP hydrologic variables.

We point out two shortcomings in our analysis. First, the 1950–2012 period of record yields a small sample size of ENSO and SIOD phase combinations, ranging from 7 EN+SIOD events to 14 LN-SIOD events. We are therefore unable to fully demonstrate sensitivity to the strength of ENSO or the SIOD or to the flavor of ENSO, as other studies have done in terms of atmosphere-only variables such as precipitation and circulation using large ensembles composed of many atmospheric model simulations (e.g., Hoell et al. 2016). Despite the small observed sample size of our study, we have confidence in our results because the average observed DJFM precipitation patterns during the ENSO and SIOD phase combinations closely correspond to average precipitation resolved in large ensembles of atmospheric model simulations forced

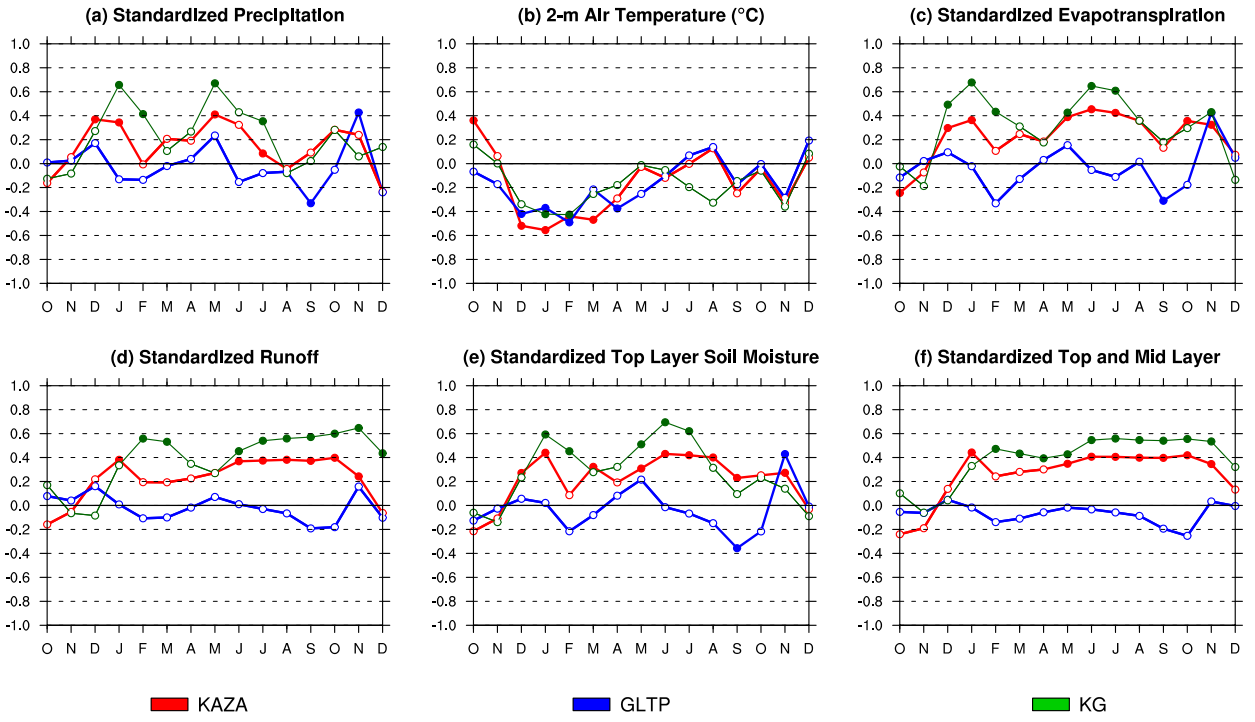

FIG. 13. As in Fig. 4, but for LN+SIOD.

by observed SSTs in Hoell et al. (2016). Second, we analyze just one hydrologic model forced by observed time-varying precipitation and temperature, the VIC model, so the conclusions that we draw in terms of the land surface hydrology could be biased toward that one model.

We do not think that the limitations of our study invalidate the conclusions reached herein, but rather recognize these possible deficiencies and identify ways to build on our current study in future work. For example, temperature and precipitation outputs from large ensembles of many atmospheric models forced by observed SSTs could be used to force various hydrologic models. Such a framework would not be biased toward individual atmospheric or hydrologic models and could be used to examine sensitivity to the strength of ENSO or SIOD or to the flavor of ENSO to create robust probabilistic scenarios of the land surface hydrology. Additionally, ensembles of coupled climate model simulations (e.g., Community Earth System Model Large Ensemble Project), which offer a large number of samples, can be used to better examine the ranges of hydrologic outcomes as forced by the comingling of ENSO and SIOD with other forms internal variability.

Improved understanding of southern Africa land surface hydrology through knowledge of the relationships between southern Africa, ENSO, and SIOD (e.g., Nicholson and Entekhabi 1986; Mason 2001; Hoell et al. 2016) will aid in the conservation and development initiatives across political borders within each TFCA (Cumming 2008; Wolmer 2003). The predictable effects of ENSO and SIOD on precipitation, temperature, and the land surface hydrology drive resource allocation (e.g., watering holes, river flows) and vegetation productivity (e.g., soil moisture, precipitation) over the growing seasons and into the dry months. The knowledge gained through improved predictability is therefore key to successful management of water, wildlife movements, human–wildlife conflict, and agricultural land-use decisions that affect the availability of various natural resources (Snyman 1998). The observed associations of how ENSO and SIOD influence the different land surface characteristics can help natural resource managers and local farmers alike with insight into the climate conditions for crops commonly grown in southern Africa and forecasts for the amount of rainfall that will then translate to water resources on the ground for wildlife (e.g., ephemeral watering holes). This knowledge will help to empower management at the local and regional scales to work in cooperation to identify both long-term policy efforts and short-term land-use decisions to sustainably manage natural resources for both conservation and development.

Acknowledgments. The authors thank Judith Perlwitz for thoughtful and constructive comments. A.H., S.S., and T.M. are grateful for the support of the Famine Early Warning Systems Network. A.E.G. is supported by National Science Foundation Geography and Spatial Sciences Grant 1560700.

REFERENCES

Ash, K. D., and C. J. Matyas, 2012: The influences of ENSO and the subtropical Indian Ocean Dipole on tropical cyclone trajectories in the southwestern Indian Ocean. *Int. J. Climatol.*, **32**, 41–56, doi:10.1002/joc.2249.

Beck, L., and T. Bernauer, 2011: How will combined changes in water demand and climate affect water availability in the Zambezi river basin? *Global Environ. Change*, **21**, 1061–1072, doi:10.1016/j.gloenvcha.2011.04.001.

Behera, S. K., and T. Yamagata, 2001: Subtropical SST dipole events in the southern Indian Ocean. *Geophys. Res. Lett.*, **28**, 327–330, doi:10.1029/2000GL011451.

——, P. S. Salvekar, and T. Yamagata, 2000: Simulation of interannual SST variability in the tropical Indian Ocean. *J. Climate*, **13**, 3487–3499, doi:10.1175/1520-0442(2000)013<3487:SOISVI>2.0.CO;2.

Chishakwe, N. E., L. Murray, and M. Chambwer, 2012: Building climate change adaptation on community experiences: Lessons from community-based natural resource management in southern Africa. International Institute for Environment and Development, 126 pp. [Available online at http://pubs.iied.org/pdfs/10030IIED.pdf.]

Colberg, F., C. J. C. Reason, and K. Rodgers, 2004: South Atlantic response to El Niño–Southern Oscillation induced climate variability in an ocean general circulation model. *J. Geophys. Res.*, **109**, C12015, doi:10.1029/2004JC002301.

Cosgrove, B. A., and Coauthors, 2003: Land surface model spin-up behavior in the North American Land Data Assimilation System (NLDAS). *J. Geophys. Res.*, **108**, 8845, doi:10.1029/2002JD003316.

Cumming, D. H. M., 2008: Large scale conservation planning and priorities for the Kavango–Zambezi Transfrontier Conservation Area. Rep. for Conservation International, 106 pp. [Available online at http://www.wcs-ahead.org/kaza/kaza_tfca_large_scale_planning_final_7nov08_logo.pdf.]

DeWeaver, E., and S. Nigam, 2002: Linearity in ENSO's atmospheric response. *J. Climate*, **15**, 2446–2461, doi:10.1175/1520-0442(2002)015<2446:LIESAR>2.0.CO;2.

Gaughan, A. E., and P. R. Waylen, 2012: Spatial and temporal precipitation variability in the Okavango–Kwando–Zambezi catchment, southern Africa. *J. Arid Environ.*, **82**, 19–30, doi:10.1016/j.jaridenv.2012.02.007.

Guan, K., and Coauthors, 2014: Terrestrial hydrological controls on land surface phenology of African savannas and woodlands. *J. Geophys. Res. Biogeosci.*, **119**, 1652–1669, doi:10.1002/2013JG002572.

Hartter, J., M. D. Stampone, S. J. Ryan, K. Kirner, C. A. Chapman, and A. Goldman, 2012: Patterns and perceptions of climate change in a biodiversity conservation hotspot. *PLoS One*, **7**, e32408, doi:10.1371/journal.pone.0032408.

Hoell, A., C. Funk, T. Magadzire, J. Zinke, and G. Husak, 2015: El Niño–Southern Oscillation diversity and Southern Africa teleconnections during Austral Summer. *Climate Dyn.*, **45**, 1583–1599, doi:10.1007/s00382-014-2414-z.

——, ——, J. Zinke, and L. Harrison, 2016: Modulation of the Southern Africa precipitation response to the El Niño Southern Oscillation by the subtropical Indian Ocean Dipole. *Climate Dyn.*, **48**, 2529–2540, doi:10.1007/s00382-016-3220-6.

Hoerling, M. P., A. Kumar, and M. Zhong, 1997: El Niño, La Niña, and the nonlinearity of their teleconnections. *J. Climate*, **10**, 1769–1786, doi:10.1175/1520-0442(1997)010<1769:ENOLNA>2.0.CO;2.

——, ——, and T. Xu, 2001: Robustness of the nonlinear climate response to ENSO's extreme phases. *J. Climate*, **14**, 1277–1293, doi:10.1175/1520-0442(2001)014<1277:ROTNCR>2.0.CO;2.

Huffman, G. J., R.F. Adler, M.M. Morrissey, D.T. Bolvin, S. Curtis, R. Joyce, B. McGavock, and J. Susskind, 2001: Global precipitation at one-degree daily resolution from multisatellite observations. *J. Hydrometeor.*, **2**, 36–50, doi:10.1175/1525-7541(2001)002<0036:GPAODD>2.0.CO;2.

——, E. F. Stocker, D. Bolvin, and E. Nelkin, 2003: Analysis of TRMM 3-hourly multi-satellite precipitation estimates computed in both real and post-real time. *12th Conf. on Satellite Meteorology and Oceanography*, Long Beach, CA, Amer. Meteor. Soc., P4.11. [Available online at https://ams.confex.com/ams/annual2003/techprogram/paper_54906.htm.]

Hughes, D. A., G. Jewitt, G. Mahé, D. Mazvimavi, and S. Stisen, 2015: A review of aspects of hydrological sciences research in Africa over the past decade. *Hydrol. Sci. J.*, **60**, 1865–1879, doi:10.1080/02626667.2015.1072276.

Hurrell, J. W., J. J. Hack, D. Shea, J. M. Caron, and J. Rosinski, 2008: A new sea surface temperature and sea ice boundary dataset for the Community Atmosphere Model. *J. Climate*, **21**, 5145–5153, doi:10.1175/2008JCLI2292.1.

Jury, M. R., C. Mc Queen, and K. Levey, 1994: SOI and QBO signals in the African region. *Theor. Appl. Climatol.*, **50**, 103–115, doi:10.1007/BF00864907.

Kalnay, E., and Coauthors, 1996: The NCEP/NCAR 40-Year Reanalysis Project. *Bull. Amer. Meteor. Soc.*, **77**, 437–471, doi:10.1175/1520-0477(1996)077<0437:TNYRP>2.0.CO;2.

KAZA TFCA, 2016: Master integrated development plan. Kavango–Zambezi Transfrontier Conservation Area, 81 pp. [Available online at http://www.the-eis.com/data/literature/Final%20Draft%20KAZA%20TFCA%20Master%20ID_June%2017%202015.pdf.]

Li, L., C. S. Ngongondo, C.-Y. Xu, and L. Gong, 2013: Comparison of the global TRMM and WFD precipitation datasets in driving a large-scale hydrological model in southern Africa. *Hydrol. Res.*, **44**, 770–788, doi:10.2166/nh.2012.175.

Liang, X., D. P. Lettenmaier, E. F. Wood, and S. J. Burges, 1994: A simple hydrologically based model of land surface water and energy fluxes for general circulation models. *J. Geophys. Res.*, **99**, 14 415–14 428, doi:10.1029/94JD00483.

——, E. F. Wood, and D. P. Lettenmaier, 1996: Surface soil moisture parameterization of the VIC-2L model: Evaluation and modification. *Global Planet. Change*, **13**, 195–206, doi:10.1016/0921-8181(95)00046-1.

Lindesay, J. A., 1988: South African rainfall, the Southern Oscillation and a Southern Hemisphere semi-annual cycle. *J. Climatol.*, **8**, 17–30, doi:10.1002/joc.3370080103.

Livneh, B., E. A. Rosenberg, C. Lin, B. Nijssen, V. Mishra, K. M. Andreadis, E. P. Maurer, and D. P. Lettenmaier, 2013: A long-term hydrologically based dataset of land surface fluxes and states for the conterminous United States: Update and extensions. *J. Climate*, **26**, 9384–9392, doi:10.1175/JCLI-D-12-00508.1.

Manatsa, D., C. H. Matarira, and G. Mukwada, 2011: Relative impacts of ENSO and Indian Ocean dipole/zonal mode on

east SADC rainfall. *Int. J. Climatol.*, **31**, 558–577, doi:10.1002/joc.2086.

——, C. J. C. Reason, and G. Mukwada, 2012: On the decoupling of the IODZM from southern Africa summer rainfall variability. *Int. J. Climatol.*, **32**, 727–746, doi:10.1002/joc.2306.

——, T. Mushore, and A. Lenouo, 2015: Improved predictability of droughts over southern Africa using the standardized precipitation evapotranspiration index and ENSO. *Theor. Appl. Climatol.*, **127**, 259–274, doi:10.1007/s00704-015-1632-6.

Marshall, M., C. Funk, and J. Michaelsen, 2012: Examining evapotranspiration trends in Africa. *Climate Dyn.*, **38**, 1849–1865, doi:10.1007/s00382-012-1299-y.

Mason, S. J., 2001: El Niño, climate change, and Southern African climate. *Environmetrics*, **12**, 327–345, doi:10.1002/env.476.

Misra, V., 2003: The influence of Pacific SST variability on the precipitation over southern Africa. *J. Climate*, **16**, 2408–2418, doi:10.1175/2785.1.

Mitchell, T. D., and P. D. Jones, 2005: An improved method of constructing a database of monthly climate observations and associated high-resolution grids. *Int. J. Climatol.*, **25**, 693–712, doi:10.1002/joc.1181.

Nicholson, S. E., and D. Entekhabi, 1986: The quasi-periodic behavior of rainfall variability in Africa and its relationship to the southern oscillation. *Arch. Meteor. Geophys. Bioclimatol.*, **34A**, 311–348, doi:10.1007/BF02257765.

——, and J. Kim, 1997: The relationship of the El Niño–Southern Oscillation to African rainfall. *Int. J. Climatol.*, **17**, 117–135, doi:10.1002/(SICI)1097-0088(199702)17:2<117::AID-JOC84>3.0.CO;2-O.

Nijssen, B., G. M. O'Donnell, D. P. Lettenmaier, D. Lohmann, and E. F. Wood, 2001: Predicting the discharge of global rivers. *J. Climate*, **14**, 3307–3323, doi:10.1175/1520-0442(2001)014<3307:PTDOGR>2.0.CO;2.

——, and Coauthors, 2014: A prototype global drought information system based on multiple land surface models. *J. Hydrometeor.*, **15**, 1661–1676, doi:10.1175/JHM-D-13-090.1.

Opdam, P., and D. Wascher, 2004: Climate change meets habitat fragmentation: Linking landscape and biogeographical scale levels in research and conservation. *Biol. Conserv.*, **117**, 285–297, doi:10.1016/j.biocon.2003.12.008.

Ratnam, J. V., S. K. Behera, Y. Masumoto, and T. Yamagata, 2014: Remote Ef FECTS of El Niño and Modoki events on the austral summer precipitation of southern Africa. *J. Climate*, **27**, 3802–3815, doi:10.1175/JCLI-D-13-00431.1.

Reason, C. J. C., 2001: Subtropical Indian Ocean SST dipole events and southern African rainfall. *Geophys. Res. Lett.*, **28**, 2225–2227, doi:10.1029/2000GL012735.

——, and D. Jagadheesha, 2005: A model investigation of recent ENSO impacts over southern Africa. *Meteor. Atmos. Phys.*, **89**, 181–205, doi:10.1007/s00703-005-0128-9.

——, R. J. Allan, J. A. Lindesay, and T. J. Ansell, 2000: ENSO and climatic signals across the Indian Ocean basin in the global context: Part I, interannual composite patterns. *Int. J. Climatol.*, **20**, 1285–1327, doi:10.1002/1097-0088(200009)20:11<1285::AID-JOC536>3.0.CO;2-R.

Rocha, A., and I. A. N. Simmonds, 1997: Interannual variability of south-eastern African summer rainfall. Part 1: Relationships with air–sea interaction processes. *Int. J. Climatol.*, **17**, 235–265, doi:10.1002/(SICI)1097-0088(19970315)17:3<235::AID-JOC123>3.0.CO;2-N.

SADC, 2016: Transfrontier Conservation Areas. Southern African Development Community, accessed 23 December 2016. [Available online at http://www.sadc.int/themes/natural-resources/transfrontier-conservation-areas/.]

Saji, N. H., B. N. Goswami, P. N. Vinayachandran, and T. Yamagata, 1999: A dipole mode in the tropical Indian Ocean. *Nature*, **401**, 360–363.

Schulze, R. E., 2000: Modelling hydrological responses to land use and climate change: A Southern African perspective. *Ambio*, **29**, 12–22, doi:10.1579/0044-7447-29.1.12.

Sheffield, J., and E. F. Wood, 2008: Global trends and variability in soil moisture and drought characteristics, 1950–2000, from observation-driven simulations of the terrestrial hydrologic cycle. *J. Climate*, **21**, 432–458, doi:10.1175/2007JCLI1822.1.

——, G. Goteti, and E. F. Wood, 2006: Development of a 50-year high-resolution global dataset of meteorological forcings for land surface modeling. *J. Climate*, **19**, 3088–3111, doi:10.1175/JCLI3790.1.

Shukla, S., J. Sheffield, E. F. Wood, and D. P. Lettenmaier, 2013: On the sources of global land surface hydrologic predictability. *Hydrol. Earth Syst. Sci.*, **17**, 2781–2796, doi:10.5194/hess-17-2781-2013.

——, A. McNally, G. Husak, and C. Funk, 2014: A seasonal agricultural drought forecast system for food-insecure regions of East Africa. *Hydrol. Earth Syst. Sci.*, **18**, 3907–3921, doi:10.5194/hess-18-3907-2014.

Snyman, H. A., 1998: Dynamics and sustainable utilization of rangeland ecosystems in arid and semi-arid climates of southern Africa. *J. Arid Environ.*, **39**, 645–666, doi:10.1006/jare.1998.0387.

Stackhouse, P. W., Jr., S. K. Gupta, S. J. Cox, J. C. Mikowitz, T. Zhang, and M. Chiacchio, 2004: 12-year surface radiation budget data set. *GEWEX News*, Vol. 14, No. 4, International GEWEX Project Office, Silver Spring, MD, 16–17. [Available online at http://www.gewex.org/gewex-content/files_mf/1476282978Nov2004.pdf.]

Tinley, K. L., 1982: The influence of soil moisture balance on ecosystem patterns in southern Africa. *Ecology of Tropical Savannas*, B. J. Huntley and B. H. Walker, Eds., Springer, 175–192.

Todini, E., 1996: The ARNO rainfall–runoff model. *J. Hydrol.*, **175**, 339–382, doi:10.1016/S0022-1694(96)80016-3.

Vörösmarty, C. J., and B. Moore, 1991: Modeling basin-scale hydrology in support of physical climate and global biogeochemical studies: An example using the Zambezi River. *Surv. Geophys.*, **12**, 271–311, doi:10.1007/BF01903422.

Washington, R., and A. Preston, 2006: Extreme wet years over southern Africa: Role of Indian Ocean sea surface temperatures. *J. Geophys. Res.*, **111**, D15104, doi:10.1029/2005JD006724.

Wolmer, W., 2003: Transboundary conservation: The politics of ecological integrity in the Great Limpopo Transfrontier Park. *J. South. Afr. Stud.*, **29**, 261–278, doi:10.1080/0305707032000060449.